CONF-790540--13

PREPRINT UCRL- 82142

Lawrence Livermore Laboratory

PLASMA CROWBARS IN CYLINDRICAL FLUX COMPRESSION EXPERIMENTS

L. J. Suter

May 18, 1979

MASTER

THIS PAPER WAS PREPARED FOR SUBMISSION TO:
THE SECOND INTERNATIONAL CONFERENCE ON MEGAGAUSS MAGNETIC FIELD GENERATION AND RELATED TOPICS, 29 May-1 JUNE 1979, WASHINGTON, D. C.

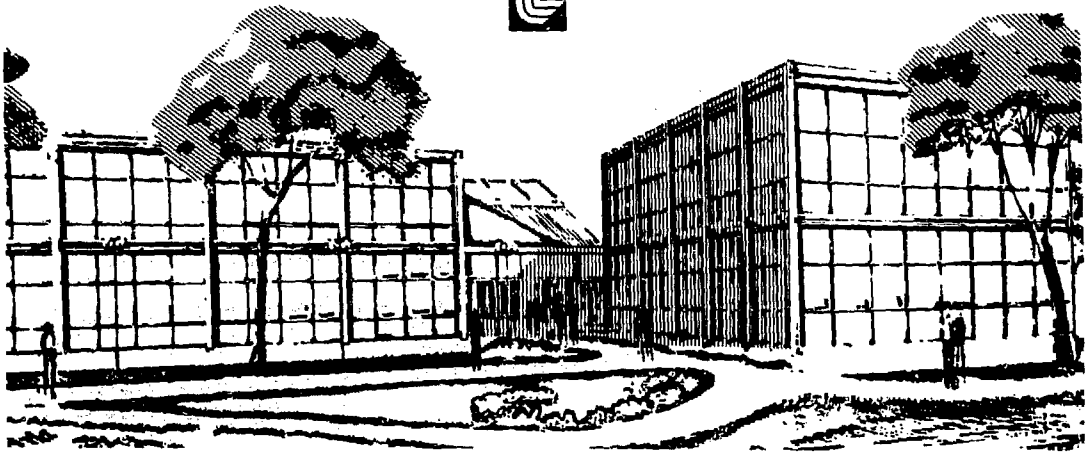

PLASMA CROWBARS IN CYLINDRICAL FLUX COMPRESSION EXPERIMENTS

L. J. Suter
University of California Lawrence Livermore Laboratory
Livermore, California

May 18, 1979

Abstract

We have done a series of one- and two-dimensional calculations of hard-core Z-pinch flux compression experiments in order to study the effect of a plasma on these systems. These calculations show that including a plasma can reduce the amount of flux lost during the compression. Flux losses to the outer wall of such experiments can be greatly reduced by a plasma conducting sheath which forms along the wall. This conducting sheath consists of a cold, dense, high β, unmagnetized plasma which has enough pressure to balance a large field gradient. Flux which is lost into the center conductor is not effectively stopped by this plasma sheath until late in the implosion, at which time a layer similar to the one formed at the outer wall is created. Two-dimensional simulations show that flux losses due to arcing along the sliding contact of the experiment can be effectively stopped by the formation of a plasma conducting sheath.

"Work performed under the auspices of the U.S. Department of Energy by the Lawrence Livermore Laboratory under contract number W-7405-ENG-48."

The Eulerian MHD code ANIMAL[1] has been used to study the experiment illustrated in Figure 1. This system is a hard-core Z-pinch with an imploding liner outer wall. In all of these simulations an external current, I_o, flows through the center rod setting up an initial magnetic field which varies as 1/r. At t = 0 there is a uniform, 20 eV D_2 plasma inside the vessel which is completely penetrated by the external magnetic field, i.e., no initial plasma currents. The moving liner has a constant, inward velocity of 1 cm/μs and may compress flux as well as the plasma. The initial size of the hard-core Z-pinch is r_{outer} = 15 cm and r_{inner} = 1 cm.

The purpose of these simulations was to study the effect of the plasma on flux compression when flux can be lost into either the center rod or the moving liner. The parameters of our study have been initial plasma density and initial external current. All other parameters (geometry, liner velocity, deuterium gas, initial temperature) were kept fixed.

One-Dimensional Simulations of Flux Loss to the Liner

One-dimensional simulations which have flux losses to the outer wall investigate implosions which have flux diffusing into the moving liner, but not into the center rod. Causes of such flux loss in a real experiment would include poor conductivity of the liner, increased flux diffusion due to late-time convergence thickening of a conducting liner, or thickening of an electrically insulating layer at late times, also due to convergence.

To specify flux loss to this outer wall ANIMAL requires us to input B(t) at the outer boundary. The code uses this B(t) to establish a $\frac{1}{r}$ "external"

magnetic field inside the container. This external field can be thought of as due to a current, I, circulating through the center rod and around the walls of the container. When no plasma is present this external field is the total field and thus the total flux in the system at a given time would depend only on the input value B(t). For our calculations we specified a B(t) at this boundary which would give a vacuum flux, ϕ_{vac}

$$\phi_{vac}(t) = \phi_o \left(1. - .75 \times \left(\frac{t}{13.7\mu s}\right)^5\right)$$

where ϕ_o is the initial flux in the system. ϕ_o can be related to an initial, circulating current I_o.

$$\phi_o = .2\ I_o \ln \frac{R_{outer}}{R_{inner}} \times \text{length}$$

I_o is a convenient parameter we use to characterize the initial flux in the system.

The way this $\phi_{vac}(t)$ should be interpreted is that at the end of the implosion (13.7 μs) we would have lost 75% of the flux in a system which had no plasma (vacuum experiment). Moreover, most of this flux loss occurs at late times. A plot of $\phi_{vac}(t)$ is shown in Figure 2.

In the presence of a plasma the total magnetic field becomes the sum of the external field and a magnetic field due to circulating plasma currents which develop during the course of the implosion. Therefore the total flux becomes

$$\phi(t) = \phi_{vac}(t) + \int B_{plasma} \cdot dA$$

This can differ significantly from the vacuum value of flux which is due to B_{ext} only.

Line b of Figure 2 is a plot of total flux vs. time for a one-dimensional simulation which had a plasma and which could lose flux to the moving liner. The initial circulating current was 1MA and the plasma density was $10^{17} cm^{-3}$. This plot shows us that the total flux inside this system at the end of the experiment is much greater than it would be if there were no plasma (vacuum experiment). The cause of this decrease in flux loss is what we call a plasma crowbar.

The plasma crowbar is a thin, very dense layer at the wall which has enough plasma pressure to support a large magnetic field gradient. It is created when flux loss causes field lines in the plasma near the wall to diffuse into the wall. This results in an imbalance of the total pressure (magnetic and material pressure) next to the wall, driving a mass flow towards the boundary. This mass flow raises the density next to the wall and also brings in more trapped field lines which diffuse out when they get near to the wall. This field diffusion provides enough heating to keep the wall plasma at a few eV temperature. The credibility of eV temperatures so near to a zero temperature wall is discussed in Appendix A.

Figure 3 shows various plasma parameters in the plasma crowbar layer vs. distance from the outer wall. This plot was made at 13.51 μs into a simulation which started with I_o = 1MA and $\rho_o = 10^{17} cm^{-3}$. We see that the plasma crowbar is cool, very dense and unmagnitized ($\omega\tau << 1$). The

thermal and electrical conductivities are their zero field values. This wall plasma supports the large field gradient which exists across this thin sheath.

This large field gradient is seen in Figure 4 which is a plot of B vs r at 13.1 μs into the simulation of Figure 3. Also shown on this graph is what B(r) would be for an implosion done without plasma. We see in the figure that there is a bump on the magnetic field profile. The rising part of this bump has been seen by Gross[2] next to a metal wall. It is due to field carried to the wall by the plasma as it experiences ∇r drift. The plasma crowbar sheath provides a boundary which, to some degree, behaves as a conducting wall.

Our physical model of the plasma crowbar says that plasma pressure on the wall holds off the magnetic field gradient. Thus, as we increase the initial current more plasma pressure will be required to hold off the increased field gradient. Since the wall temperature will remain low ($K \alpha T^4$), more density is required at the wall to balance the field pressure. In order to raise the wall density more mass must come from the interior of the vessel. This additional mass will drag more flux with it which will be lost to the liner. Thus our model says that higher initial current should result in a greater fraction of the flux being lost.

Figure 5a is a plot, for several initial currents, of the fraction of flux left at the end of the experiment vs. fill density. Inspection of these curves at fixed density shows that the fraction of flux conserved by the plasma

crowbar decreases with increasing initial current. Figure 5b is a plot of the mass fraction not jammed against the wall at 13.0 μs vs. initial current. As I_o is raised, more of the plasma is consumed by the plasma crowbar. These results are consistent with our model.

Finally we observe that our model implies that at fixed current more initial density should require a smaller fraction of total mass to flow to the wall in order to balance the field gradient. This means that raising density should reduce the amount of flux lost due to formation of the plasma crowbar. Figure 5a shows this to be true.

One-Dimensional Simulations with Flux Loss into the Center-Rod

These calculations attempt to simulate an experiment in which flux is lost into the center-rod. The most obvious reason for such losses in a real system is dissipation due to the large current densities that might be carried by this conductor.

Qualitatively, one expects the same results for flux loss into the rod as were found for flux lost into the liner. Flux loss should drag mass to the rod which increases the pressure and tends to support a field gradient. However, quantitatively we find that over most of the implosion not enough mass goes to the rod to generate an effective plasma crowbar.

This observation can be understood with the aid of Figure 6. This figure is a plot of mass fraction dragged to a boundary vs. the fraction of flux lost through that boundary. This plot is for a simplified experiment, similar to Figure 1, which does not have a moving outer wall but does lose flux into either the outer wall or into the center-rod. The particles are assumed to be frozen to field lines.

What we see is that when $R_{outer} >> R_{inner}$ a small amount of flux loss to the outer wall is accompanied by a large fraction of the total mass. Thus loss to the outer wall can drag lots of material for creating a plasma crowbar.

On the other hand, flux loss to the inner wall of the same system is accompanied by very little mass. We may not collect enough mass to generate a plasma crowbar on this boundary.

The physical reason for this difference is that the particles are mostly at large radius while the flux is concentrated at small radius.

$$\delta N = 2\pi r \rho \delta A$$

$$\delta \phi = \frac{.2I}{r} \delta A$$

Therefore $$\frac{\delta N}{\delta \phi} = \frac{10\pi r^2 \rho}{I}$$

At 15 cm there are 225 times the particles/unit flux as there are at 1cm.

Also plotted in Figure 2 is the flux vs. time for a lossy rod simulation. We see that it is close to the vacuum value over most of the experiment, deviating from the vacuum value only at late times. What is happening is that throughout the implosion a cold, dense plasma layer is being formed along the center rod. However, there is not enough mass in this layer to create an effective plasma crowbar until very late in time.

There are two reasons for the eventual, late-time formation of the plasma crowbar. First our flux loss model dictates that most of the flux is lost at late times. Second, the outer radius is no longer large compared to the inner radius. Therefore, the mass fraction which accompanies a given amount of flux loss is now much greater (Figure 6). It turns out that at late time we can form an effective plasma crowbar along the center conductor. This is seen in Figure 7 which is a plot of total magnetic energy vs. time for three cases - vacuum, plasma with losses to outer wall and plasma with losses to the inner wall. We see from this curve that the plasma crowbar becomes effective for losses to the rod only at very late times.

Since the mechanism for forming the plasma crowbar on the inner conductor is the same as the mechanism for forming it on the outer wall, we would expect the dependence upon fill density and initial field to also be the same. This is supported by Figures 8a and b. Figure 8a shows the time at which the plasma crowbar becomes effective vs. fill density. This time is defined as the instant when the field energy of Figure 7 turns up. Raising the density makes the crowbar come earlier while increasing the field delays it. Figure 8b shows the fraction of flux left vs. fill density. It goes down at very high densities because $\omega\tau$ is everywhere less than 1 and the plasma rapidly cools to the point where it is no longer tied to the field lines. Radiation losses in these high density simulations do not seem to be the dominant factor in the failure of the plasma crowbar at high ρ_o.

Two-Dimensional Calculations

Several two-dimensional calculations were done on the hard-core Z-pinch system to see if two-dimensional effects change the one-dimensional results. No significant differences were found. Figure 9 is a two-dimensional plot of current density for a system which loses flux to the outer wall. The fill density was $10^{17} cm^{-3}$ and the initial current 1MA. Figure 9 clearly illustrates the very large plasma crowbar current flowing along the outer wall. Just inside this region is a smaller current in the reverse direction. This reverse current is due to the bump on the magnetic field vs. radius shown in Figure 4. The flux vs. time for this system is shown in Figure 2. This curve is virtually identical to the one-dimensional result. It appears that two-dimensional effects do not significantly modify the plasma crowbar.

Finally, we did two-dimensional calculations which attempted to simulate a cylindrical system which has arcing at the sliding contacts between the moving liner and the conducting end plates. To simulate these arcs we allowed the system to lose flux only at the ends of the liner. Figure 10 shows the current distribution at 13 μs for an experiment which started at $\rho_o = 3 \times 10^{17} cm^{-3}$ and $I_o = 1MA$. We see a very large plasma current at the simulated arc. This is the plasma crowbar current which appears to be very effective in this experiment. The flux vs. time for this simulation is plotted in Figure 2. It had the smallest fractional flux loss of all our simulations.

Conclusions

These one- and two-dimensional simulations indicate that the presence of a plasma in a hard-core Z-pinch flux compression experiment can significantly enhance the final magnetic field achieved by the system. The degree of enhancement depends upon initial field, plasma density and whether the loss is to the inner wall or the outer wall.

It appears that flux losses into the moving liner or into an arc at the sliding contact will be greatly reduced by the formation of the plasma crowbar. This may be important because it indicates that good sliding contact and high conductivity pusher materials are not crucial for the success of such a flux compression. It also may be important because it further indicates that in plasma-implosion experiments the liner need not be a good conductor. Over a wide range of fields and densities the material may be chosen due to considerations other than a need for high electrical conductivity. Specifically, one could consider using an outer wall of a refractory insulator.

Losses into the center-rod are not reduced until very late in time when the plasma has been pushed close to the rod where the flux is concentrated. Thus the plasma crowbar, while interesting, will not be nearly as effective in enhancing the flux compression of a system with losses into the center-rod.

Appendix A

One result which should be questioned is the huge temperature gradient which must exist near the wall if this plasma crowbar is to be real. In order to form a plasma crowbar we need the plasma temperature to rise from the wall temperature to a few eV within several microns (see Figure 3). This appears to be an extremely steep gradient. However, we believe it's real for two reasons.

First, the ANIMAL results converge as we put finer and finer zones next to the wall. Figure 11 shows T(r) for two different zonings at $\rho_o = 3 \times 10^{16} cm^{-3}$ and $I_o = 2MA$. The data points show the locations of the zone centers for each calculation. The resulting T(r) profiles are nearly the same, indicating that the calculations have converged on a consistent solution of the code's physical model.

The second reason for believing the temperature profile is that it is not as steep as it could be if one considered thermal conductivity alone. If we neglect radiation, PdV, and ohmic heating, then energy conservation takes the form

$$\frac{\partial}{\partial r} K(t) \frac{\partial T}{\partial r} = n C \dot{T}$$

We would want $\dot{T}$ to be $\gtrsim 0$ at the wall if the plasma is not to collapse. Using Spitzer conductivity we find that this requires

$$\frac{5}{2} \left(\frac{\partial T}{\partial r}\right)^2 + T \frac{\partial^2 T}{\partial r^2} \gtrsim 0 \quad .$$

This implies that there is some maximum downward curvature in the temperature profile which will not require a local energy source to prevent cooling. This maximum curvature profile is

$$T(r) = T_o + c\, r^{0.286}$$

This profile is also plotted in Figure 11 where one end point has been tied to the interior plasma temperature. Comparing this T(r) to the one calculated by the code, we see that the calculated value does not have as much curvature as it could have. The wall thermal gradient, while steep, is not as steep as it could be. In absence of any other effects (which are considered by the code) the thermal gradient would actually steepen. Thus we are willing to believe the code when it predicts eV temperatures a few microns from the wall.

References

1. I. Lindemuth, "The ANIMAL Code," Lawrence Livermore Laboratory report, UCRL 52492, (1979).

2. R. A. Gross, Nuclear Fusion, 15, 729-735, (1975).

Figures

Figure 1 - Geometry used for all of our calculations. A hard-core Z-pinch of 1 cm inner radius and 15 cm initial outer radius. The liner implodes at 1 cm/μs. There is an initially uniform D_2 plasma at 20 eV temperature inside the container. At the start of the implosion the circulating current, I_o, creates a magnetic field which fully penetrates the plasma.

Figure 2 - Flux vs. time for several systems.

a) Vacuum, b) 1-D with flux loss to the liner, $10^{17}cm^{-3}$, 1MA

c) Same as b except 2-D calculation, d) 1-D with flux loss to rod, $10^{18}cm^{-3}$, 1MA, e) 2-D with arc losses at the ends, $10^{17}cm^{-3}$, 1MA.

Figure 3 - Plasma crowbar sheath parameters at 13.57 μs vs. distance from the liner for a flux loss to the liner calculation which started at $10^{17}cm^{-3}$, 1MA.

Figure 4 - B vs r at 13.1 μs for a simulation which started at $10^{17}cm^{-3}$ and I_o = 1MA. The lower curve is B(r) for a vacuum.

Figure 5 - a) Fraction of flux remaining at 13.7 μs vs. N_o for several initial currents. Loss to liner.

b) Fraction of mass not consumed by the plasma crowbar at 13.0 μs vs. initial current.

Figure 6 - Fraction of total mass dragged to a boundary vs. fraction of flux lost thru that boundary. Non-imploding system with material frozen to field lines. The two outer curves are for $R_{outer}/R_{inner} = 15$ while the inner curves are for $R_{outer}/R_{inner} = 1.7$.

Figure 7 - Total magnetic energy vs. time for a) vacuum, b) plasma with loss to the center rod, c) plasma with loss to the liner. Initial plasma density $3 \times 10^{17} cm^{-3}$ and $I_o = 1MA$.

Figure 8 - a) Time of plasma crowbar vs. fill density at two initial currents. Loss to the center rod.

b) Fraction of flux left @ 13.7 μs vs. fill density for two initial currents. Loss to the center rod.

Figure 9 - Current density at 13.0 μs for a 2-D calculation with flux loss to the liner. The large current flowing next to the liner is the plasma crowbar current. The smaller current just inside the plasma crowbar flowing in the reverse direction produces the bump on the B(r) profile seen in Figure 4.

Figure 10 - Current density at 13.0 μs for a 2-D calculation with flux loss due to arcs at the sliding contact. The large current at the upper right is the plasma crowbar current. The smaller, reverse current along the conducting liner results from the rise in B vs. r that one gets at a conductor from $\nabla r\ drift^2$.

Figure 11 - Temperature vs. distance from the liner at 13 μs for two different zonings of the same problem. I_o was 2MA & $\rho_o = 3 \times 10^{16} cm^{-3}$. The points are located at the zone centers. Also shown is the temperature profile that would exist if the interior point were held at 30 eV and thermal conduction to the zero temperature wall were the only energy loss mechanism in the plasma sheath. Thermal conduction alone will support a much steeper temperature gradient than is needed to create a plasma crowbar.

Figure 1

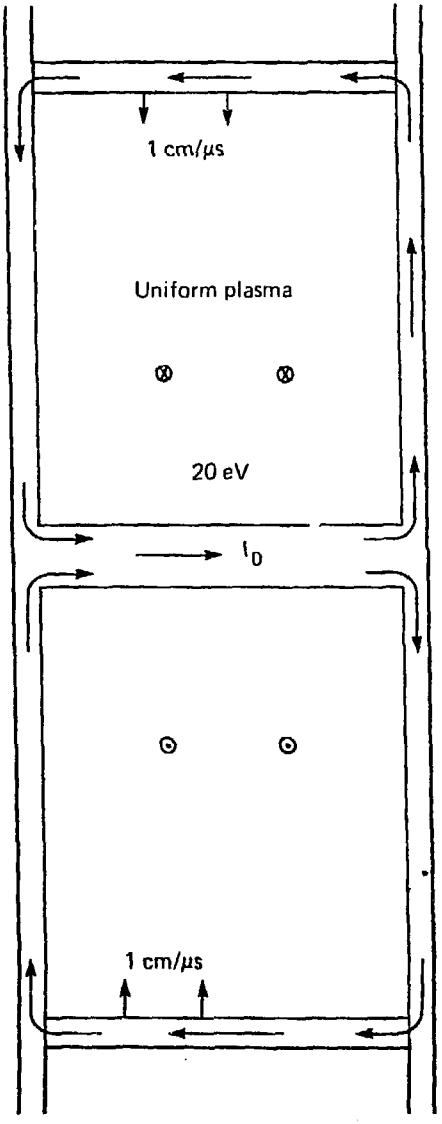

Figure 2

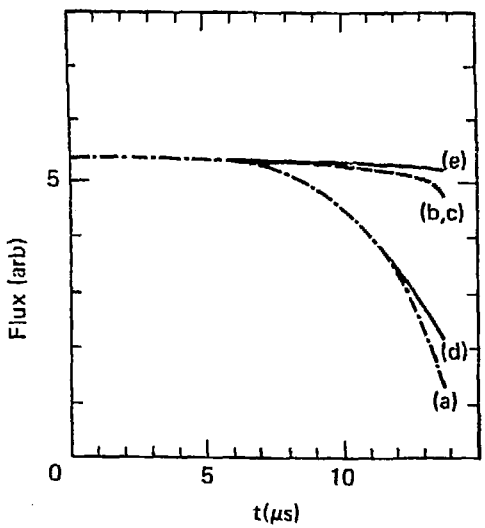

Figure 3

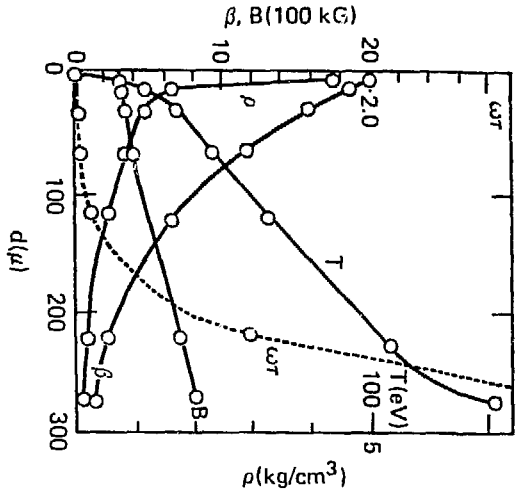

Figure 4

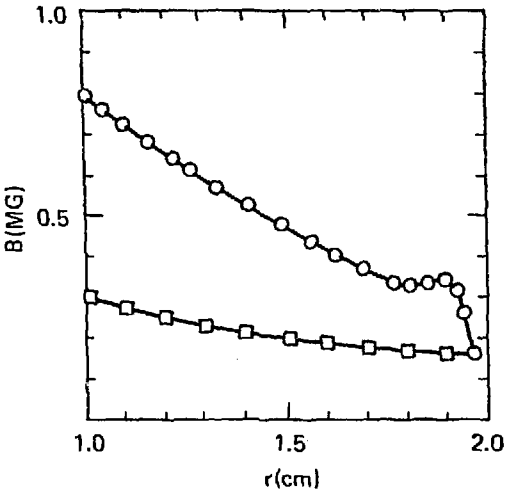

Figure 5

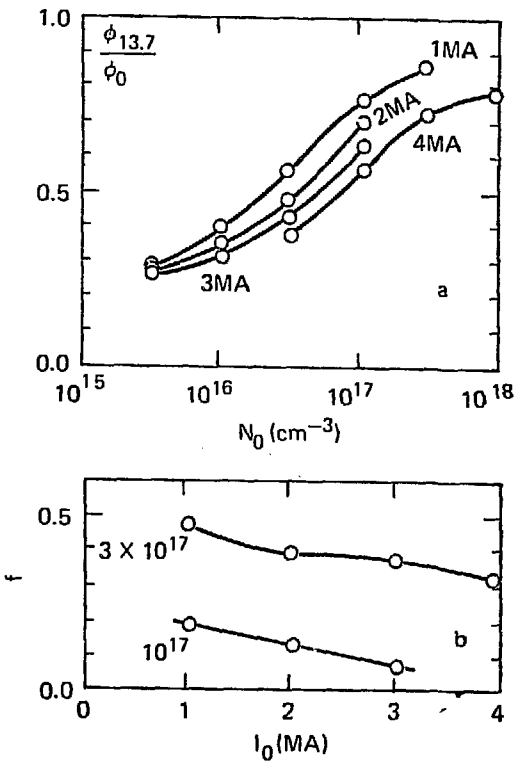
1.0
0.5
0.0
$\frac{\phi_{13.7}}{\phi_0}$
1MA
2MA
4MA
3MA
a
10^{15}
10^{16}
10^{17}
10^{18}
N_0 (cm^{-3})
0.5
0.0
f
3 X 10^{17}
10^{17}
b
0
1
2
3
4
I_0(MA)

Figure 6

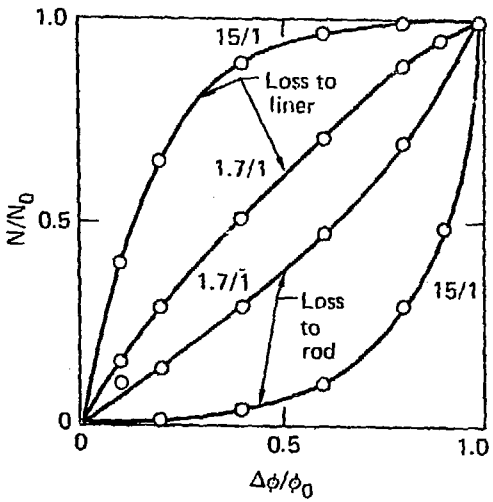

Figure 7

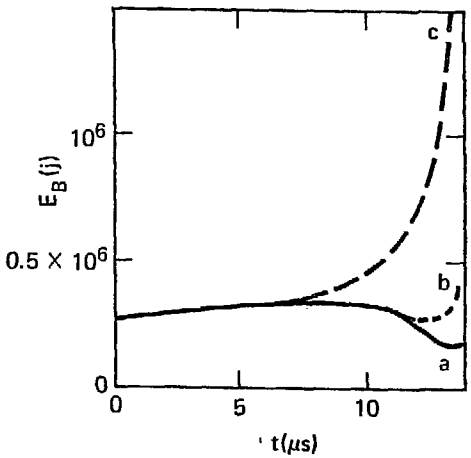

Figure 8

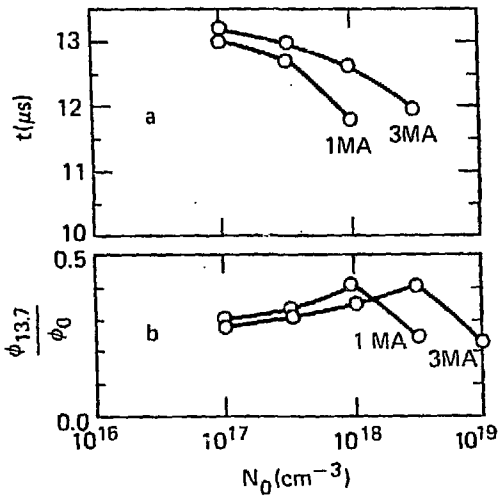
13
12
11
10
t(μs)
a
1MA
3MA
0.5
0.0
$\frac{\phi_{13.7}}{\phi_0}$
b
1 MA
3MA
10^{16}
10^{17}
10^{18}
10^{19}
$N_0(cm^{-3})$

Figure 9

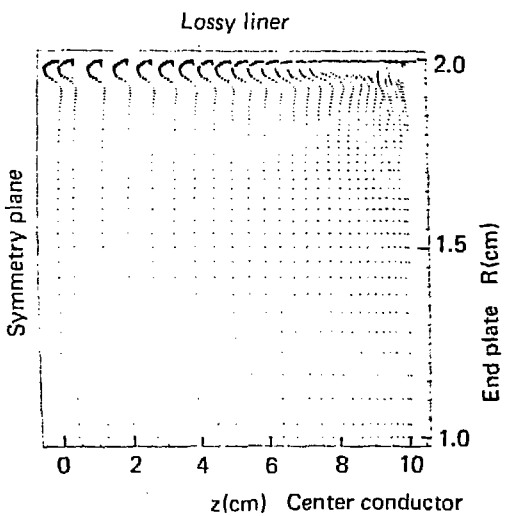
Lossy liner
2.0
1.5
1.0
Symmetry plane
End plate R(cm)
0
2
4
6
8
10
z(cm) Center conductor

Figure 10

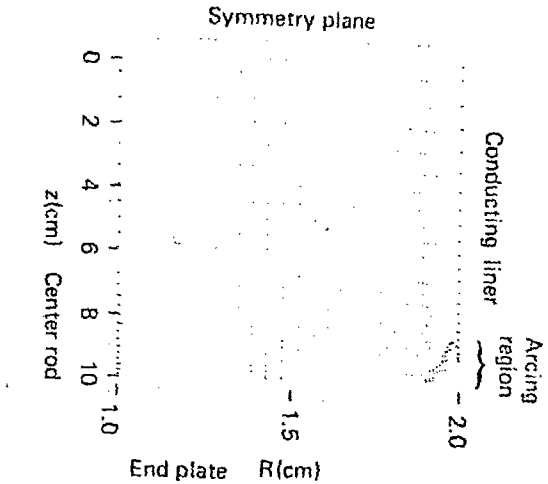
Symmetry plane
Conducting liner
Arcing region
0
2
4
6
8
10
z(cm)
Center rod
1.0
1.5
2.0
End plate
R(cm)

Figure 11

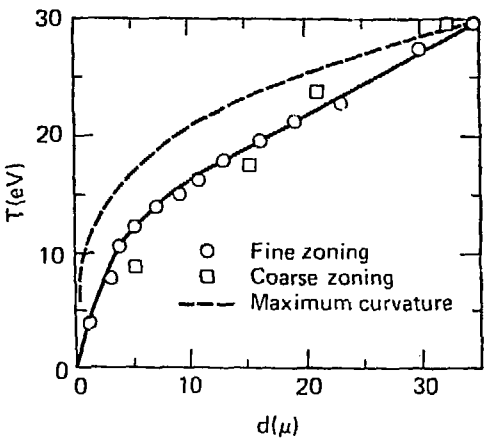
30
20
10
0
T(eV)
0
10
20
30
d(μ)
Fine zoning
Coarse zoning
Maximum curvature